

SYNTHETIC JET THRUST OPTIMIZATION FOR APPLICATION IN UNDERWATER VEHICLES

Michael Krieg, Christopher Coley, Christopher Hart, and Kamran Mohseni

Department of Aerospace Engineering,
University of Colorado, Boulder, Colorado 80309-429

Abstract—Zero-mass pulsatile jets are proposed for low speed maneuvering and station keeping of small underwater vehicles. The flow field of such jets are initially dominated by vortex ring formation. Such pulsatile jets can be actuated through a variety of techniques. Two prototypes of such actuators, presented here, include a mechanical plunger system and a solenoid actuator. The actuators consist of a small cavity with an orifice on one side and a moving diaphragm on the other side. Oscillation frequencies are varied between zero and 40 Hz for the mechanical plunger and upto 50 Hz for the solenoid actuator. The mechanical actuator is designed so that the cavity dimensions, orifice diameter, actuation frequency, and actuation profile can be easily varied in order to find the optimal operation point of the actuator. Thrust measurement data is provided for various formation numbers while the actuation frequency is varied. The empirical thrust profiles were seen to follow the same trend as a model previously developed by our group. It is also observed that the measured thrust has a maximum value for formation numbers between 4 and 5.5 for various actuation frequencies and for two different cavity diameters. Solenoid actuation shows an almost linear stroke dependency on the actuation frequency.

I. INTRODUCTION

Marine excavation (especially deep sea excursion) has taken great strides recently with the advent of advanced sensing techniques as well as highly controllable remotely operated vehicles (ROVs). Most ROVs need significant logistic support, such as escort ships, that could limit their availability to the general research community. Furthermore, the required cable connection has limiting effects on ROVs operation, in particular in deep oceans. Ultimately, as these vehicles requirements become increasingly demanding, their limitations will become mission critical. Therefore, self-propelled autonomous underwater vehicles (AUVs) will become increasingly important in the commercial realm. Such autonomous vehicles are expected to require less technical and logistic support, and will be capable of operating in regions into which no manned underwater vessel or ROV could penetrate (e.g., below the ice regions and to the bottom of trenches).

Hydrodynamic design of AUVs are often driven on a few competing fronts: (i) Rapid and efficient deployment to the work-zone and (ii) low speed maneuvering during the docking procedure and for operations at the work-zone. Rapid deployment necessitates a streamlined body of revolution (e.g. Torpedo-shape design) for fast cruising with minimal energy.

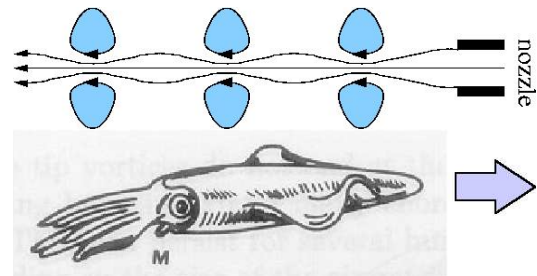


Fig. 1. Squid locomotion by pulsed jet.

However, since the trajectory of this type of vehicles is adjusted using control surfaces, the magnitude of the available control force is proportional to the vehicle's speed. Consequently, these vehicles are difficult to maneuver at low speeds and in tight spaces. Therefore, they are difficult to dock or maneuver through sunken excavation sites. Such vehicles also cannot opportunistically enter a precise loitering or hovering mode. As a result much current effort is devoted to the development of docking mechanisms, but this is just a solution for the symptoms, and does not really address the problem of the vehicle's actual maneuvering capabilities.

On the other hand, low speed maneuvering and better control are often achieved by the so-called box-design where the low drag body-of-revolution design is sacrificed by adding multiple thrusters at different locations and directions. In this case, precise maneuvering can be achieved at the cost of increased drag and the need for an alternate technique to transport the vehicle from the offshore base or an escort ship to the work-zone.

In an effort to resolve this trade-off, recent proposals have been made to use compact synthetic jets for low speed maneuvering or locomotion of small unmanned underwater vehicles (UUVs) [1], [2]. The propulsion scheme suggested here is loosely inspired by the propulsion of cephalopods and jellyfish [3], [4], [5], [6], [7], [8]. Squid (see Figure 1) use a combination of fin undulations and a jet which can direct thrust at any angle through a hemisphere below the body plane. Jet locomotion of the squid is accomplished by drawing water into the mantle cavity, and then contracting the mantle muscles to force water out through the funnel. The funnel, which is directly behind and slightly below the head,



Fig. 2. Cylinder piston mechanism.

can be maneuvered so as to direct jets in a wide range of directions. Since nature has had thousands of years to optimize this actuation technique, these basic parameters are an ideal starting position for our own optimization. Another example of pulsatile jet locomotion is jellyfish swimming [9], [10], which relies upon repeated contractions of an umbrella-shaped structure, or bell.

Weihs [8], Seikman [6], and recently Krueger and Gharib [11], [12] have shown that a pulsed jet can give rise to a greater average thrust force than a steady jet of equivalent mass flow rate. In a pulsed jet, an ejected mass of fluid rolls into a toroidal vortex ring which moves away from its source. A continuously pulsed jet, therefore, produces a row of vortex rings (see Figure 1). At high pulsing frequency, the jet structure can become increasingly turbulent and irregular.

A variety of mechanical drivers can be employed to oscillate the pressure within a cavity necessary to generate vortex ring jets. A cylindrical cavity can be contracted and expanded changing its volume very similar to biological methods. However, a much simpler design, suitable for laboratory experiments, would keep a constant sized cavity and use an internal piston to drive the pressure variations; the so-called cylinder-piston mechanism (see Figure 2). When the piston pushes fluid through the cylinder, the boundary layer of the fluid expelled from the cylinder will separate and roll up into a vortex ring at the orifice edge. Experiments [13] have shown that for large enough ratios of piston stroke versus diameter (L/D), the generated flow consists of a leading vortex ring followed by a trailing jet.

This paper considers thrust characteristics of a synthetic jet actuator (see Figure 3) for application in underwater vehicle locomotion and maneuvering. A Cylinder-piston mechanism was traditionally used for starting jets. This system provides a simplified approximation to natural pulsatile jet generation, and is amenable to experimental, computational, and analytic study. A starting jet is usually characterized by the roll up of the ejected shear layer from a nozzle or an orifice and the formation of vortex rings. The generation, formation, evolution, and interactions of vortex rings have been the subject of numerous investigations (see, *e.g.* Shariff and Leonard [14] and the references in there). In this study, we focus our attention on a specific characteristic of vortex ring formation; namely the impulse extremization in vortex ring formation and its connection with the vortex ring pinch-off phenomenon.

While the piston-cylinder model is attractive for theoretical studies and ease of experimental set-up, there are more practical means to generate pulsatile jets. To this end, prototypes of pulsatile jet generators using the Helmholtz cavity concept are designed and built [1], [2]. Various techniques can be

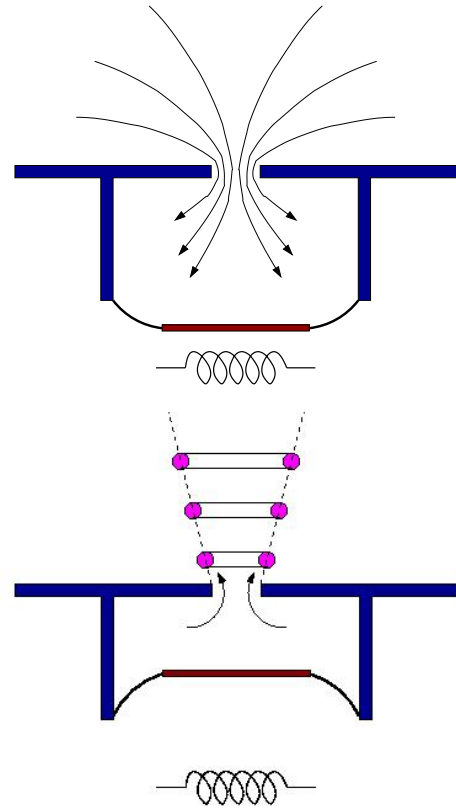


Fig. 3. Synthetic jet actuator concept: (Top) Fluid entrainment; (Bottom) vortex ring formation.

employed for actuating the diaphragm. These includes, but are not limited to, using electromagnetic actuations (*e.g.* solenoid plungers), electrostatic and piezoelectric actuation. In this design the inward movement of a diaphragm draws fluid into a chamber (Figure 3). The subsequent outward diaphragm movement expels the fluid, forming a vortex ring or a jet depending on the formation number. Repetition of this cycle results in a pulsatile jet. Because of the asymmetry of the flow during the inflow and outflow phases, a net fluid impulse is generated in each cycle, even though there is no net mass flow through the chamber over one cycle. For a more in depth consideration of the net mass and momentum flux in this regime see Mittal *et al.* [15].

Figure 4 shows the structure and appearance of a pulsatile jet actuator prototype [16], [17] built in our group. The driving diaphragms consist of a rigid disk with a flexible surround. The diaphragm can be actuated by electrical, mechanical, or magnetic actuations. Currently a solenoid actuator is used to generate the diaphragm motion. The fluid pushed by the moving diaphragm exits through an orifice. Ultimately the optimal parameters discovered in this research will drive the design constraints on this prototype for use in AUV maneuvering. This design has many advantages including its simplicity, very few moving parts, and compactness. This study aims not only to examine the optimal characteristics of ring formation (from an impulse standpoint), but to also examine the capabilities and limitations of several types of actuation techniques. To that extent two types of actuators were used during testing.

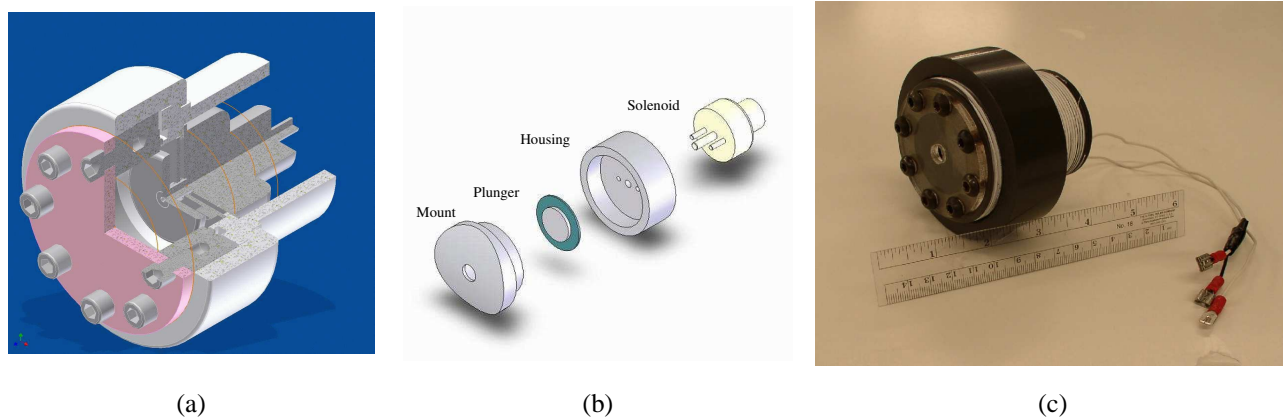


Fig. 4. CU Boulder Synthetic jet prototype [16], [17]: (a) CAD model of the actuator design. (b) Plunger and solenoid assembly. (c) Actual fabrication of the synthetic jet actuator.

One was a mechanically driven actuator used to study the defining characteristics related to impulse extremization. The other is a smaller solenoid driven actuator, used for visualizing the flow regime of the ring vortex, as well as determining the limitations which will be imposed on any compact driving system. The combination of the parallel forms of analysis will ultimately allow for the design of theoretical optimal actuation parameters as well as those optimal parameters which apply to more typical actuation techniques. Voice coil actuation results are presented in [18] in this proceeding and in [19].

Mohseni [1], [2] offered a model to predict the impulse of vortex ring jets with varying parameters in a synthetic jet. This investigation is focused on direct measurement of thrust in a synthetic jet while the actuation frequency and the formation numbers are varied. Remotely controlled underwater vehicles designed to incorporate these actuators, and prove their ability to provide control forces have been built and tested at the University of Colorado at Boulder. Two such vehicles are shown in Figures 5 and 6. In particular the location of the synthetic jet actuators are shown in Figure 6. It should be noted that our proposed technique does not have any protruding part to affect the performance of the vehicle at higher cruising speeds.

The newer vehicle shown in Figure 6, known as the Remote Aquatic Vehicle (RAV), houses four Synthetic Jet Actuators (SJA's). The actuators used in the RAV produce thrust with a solenoid type of actuation. An exploded view of the actuator is shown in Figure 4.

II. EXPERIMENTAL SETUP

The experimental apparatus used for this investigation, is comprised of two separate systems. These include both a thrust measurement system, used for investigating actuator characteristics, as well as a stroke measurement system, which characterizes the limitations of a more typical (solenoid) actuator under various loads and running conditions.

A. Thrust Measurement Setup

Schematic of the thrust measurement system is shown in Figure 7. The actuator is submerged in large tank of water

(weighted to be neutrally buoyant) and suspended by a plate which restricts all horizontal motion. The vertical motion was driven by the vortex jet impulse transfer, and measured by a load cell mounted on the plate, in contact with the actuator.

The actuator itself is driven by a mechanical plunger system. The motor's rotational motion is translated to a linear oscillation through a cam mechanism. The plunger consists of a cylindrical accordion shaped bellows, which oscillates up and down inside the Helmholtz cavity. Though solenoid-diaphragm actuation systems (considered in Mohseni [2], [1]) have many benefits in vehicle applications (mainly due to their compact size), we found that a better controlled experiment can be conducted with our mechanical plunger driven by a motor to find the optimal operation zone of a synthetic jet. In an optimization process it is necessary to maintain close controls, in order to accurately observe the effect of parameter variation. It was in this respect that a mechanical plunger system was found useful. For example a major focus of our experiment was to quantify the effect of adjusting the formation number of the expelled jet. In order to accomplish this a very accurate control of the formation number is required. If the jet volume were to remain constant, the control over the formation geometry would be a simple matter of adjusting the orifice diameter. With a solenoid setup the deflection of the diaphragm is a function of the load, causing the jet volume to vary with frequency. The mechanical plunger; however, has a stroke length completely determined by the geometry of the cam, allowing for a constant volume and easily controllable formation number. Additionally the mechanical plunger setup allows the piston to be placed in Helmholtz cavities of any geometry, allowing even greater control over the design parameters during experimentation. Once the optimal characteristics have been determined they can then be adapted to a simpler solenoid design, which has more benefits in vehicular application.

The current mechanical plunger system have the capability of changing the following parameters in a synthetic jet actuator

- plunger stroke
- plunger velocity profile
- plunger frequency
- orifice height and diameter



Fig. 5. University of Colorado Test Beds. The smaller vehicle is equipped with 4 synthetic jet actuators.

- cavity height and diameter
- other geometrical parameters of the cavity

In this paper we will focus on varying the orifice diameter, actuation frequency, and cavity diameter.

This entire mechanical system was placed in a PVC canister (to make it water tight) and submerged in the water tank. The setup was used to acquire two sets of data; the first is the actual thrust output from the actuator which is processed by the computer from the load cell voltage output. The second is the rotation frequency of the motor which is processed by the computer from the motor encoder pulse count, translated and filtered through an HP universal counter.

B. Solenoid Stroke Measurement Setup

A solenoid driven actuator was created to simulate typical actuators for use in small underwater vehicles. Solenoid's stroke is a function of its loading. The achieved stroke of the solenoid dictates the volume of fluid that is expelled through the actuator's orifice. Thus it is important to characterize the solenoid displacement under operating conditions in order to design a final solenoid actuator which operates at its optimal working parameters.

In order to measure the displacement of the solenoid, the synthetic jet actuator is mounted horizontally to a plate with an orifice through which fluid can pass. The system can be seen in Figure 9 below. The solenoid is activated by a square voltage signal at the desired frequency. A linear potentiometer is attached to the rear of the solenoid to measure the position of the plunger as it operates in the fluid. This apparatus allows for many design parameters to be changed, including orifice diameter, membrane thickness, and actuation frequency.

III. RESULTS AND DISCUSSION

In this section data for thrust measurement and solenoid stroke are presented.

A. Thrust Maximization Characteristics

The described setup in Figure 7 was driven at various test conditions. The orifice was adjusted such that the formation number (L/D , see Figure 2) varied between 2 and 8 (with higher sensitivity around L/D of 4). This parameter could be easily controlled since a mechanical plunger system forces the jets to maintain a constant volume at each stroke. For each formation number the motor was adjusted to run between frequencies of 0 and 40 Hz. Each arrangement generates a thrust response curve in the time domain. It should be noted that the response curve is comprised of several smaller waveforms each containing 300 thrust samples for a single oscillation frequency value. The sum of these waves over the entire frequency domain of the experiment represents a complete description of the specific formation number's response. Two examples of these smaller waveforms (taken with a formation number 3.93) are depicted in Figures 10 and 11.

The thrust curve can be seen to have an average thrust value above the offset; in fact at higher frequencies the entire curve is above the offset, verifying the ability of the actuator to create a sustainable thrust. Each of these single frequency sections can then be averaged to find a mean, sustainable thrust pertaining to the section's specific oscillation frequency. Using this type of analysis, the thrust response curve can be depicted in the frequency domain rather than the time domain, which is much more relevant to the optimization of the actuator. In an effort to incorporate the forces lost to dynamic effects an inertia correction factor was calculated and included to take into account the acceleration of our system. A typical thrust response curve in the frequency domain is shown in Figure 12 for $L/D = 3.93$. As predicted in Mohseni [1], [2] the expected thrust shows a dependency to the square of the actuation frequency. A second order polynomial fit to the experimental data is also shown in Figure 12. Fitted curves to

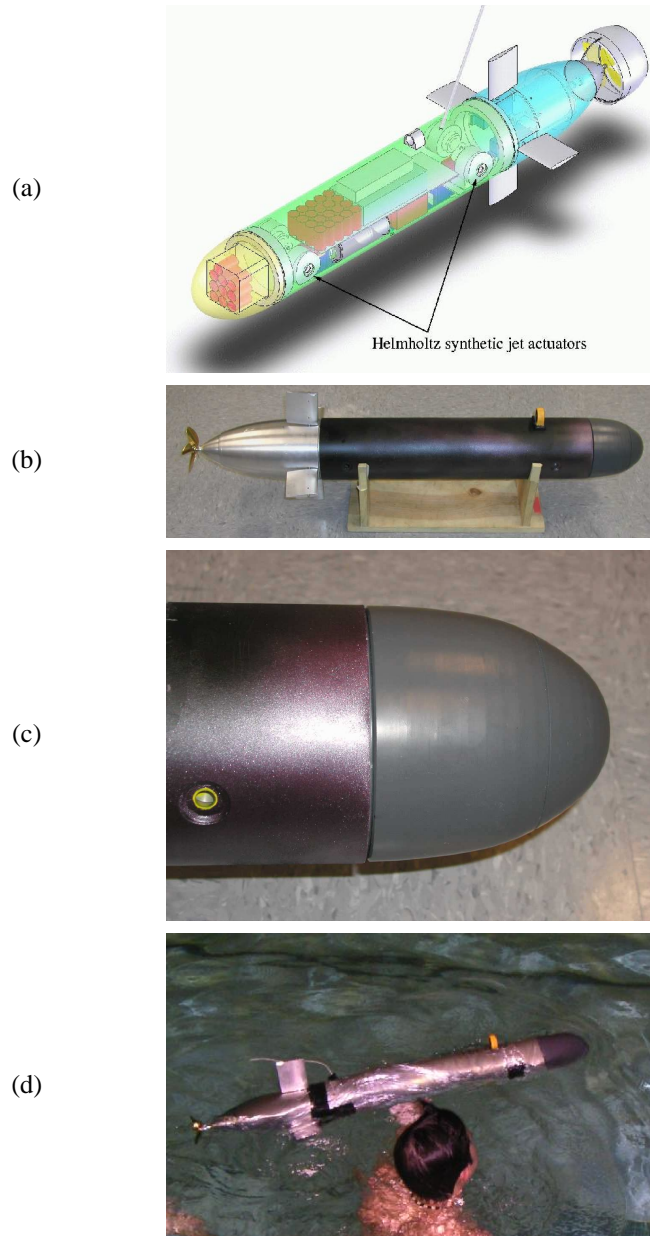


Fig. 6. UUV test bed at the University of Colorado. (a) CAD model of the Colorado UUV with SJAs. (b) Colorado UUV. (c) Exit orifice of the SJA on the Colorado UUV. (d) Testing of the Colorado UUV in the pool.

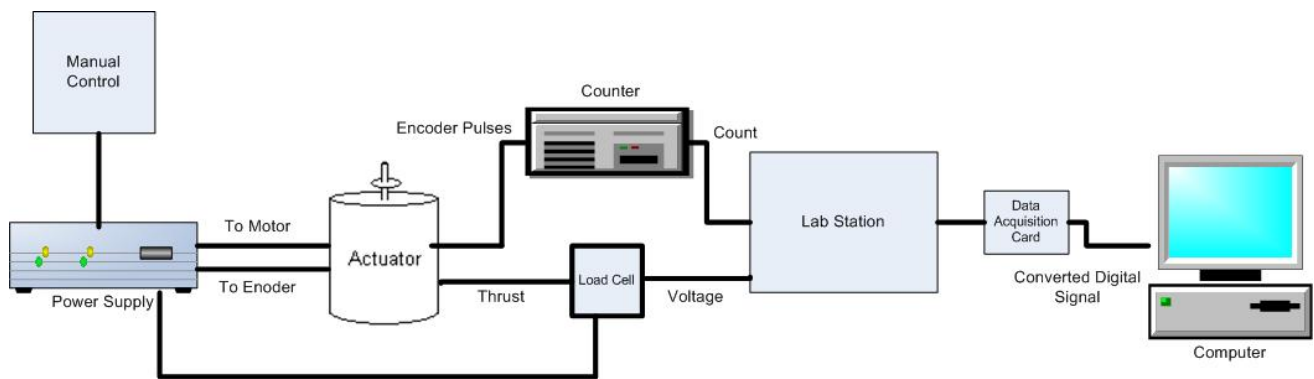
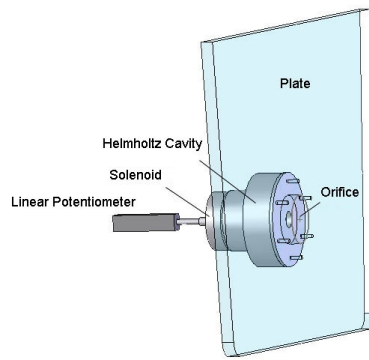


Fig. 7. Schematic of the experimental setup for thrust measurement.



(a)

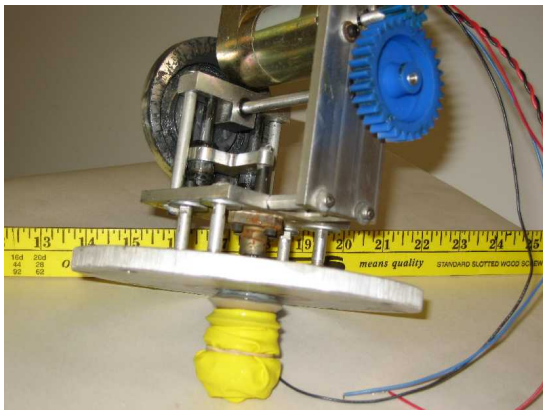


(b)

Fig. 9. Stroke measurement apparatus (a) Typical solenoid actuator (b) Sensor orientation

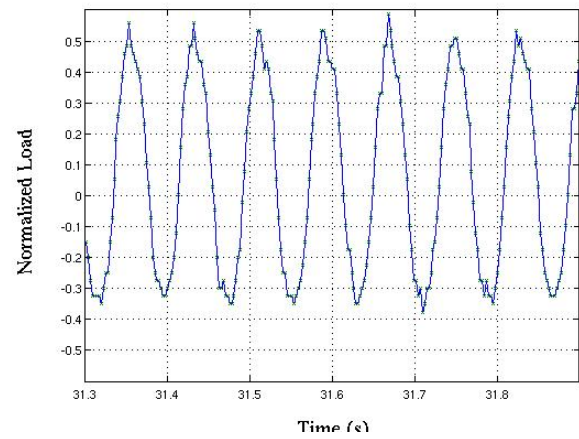


(a)



(b)

Fig. 8. Mechanical plunger setup (a) motor, gear and cam assembly. (b) Piston/plunger inside the cavity.



g

Fig. 10. Normalized load at 11 Hz actuation.

the experimental data for other formation numbers are shown in Figure 13, where the same dependency on frequency is observed. It is clearly seen that the maximum thrust at most frequencies is achieved for formation numbers around 4-5.5.

Figure 13 is useful in recognizing the response of the actuator due to increased frequency, but it is difficult to discern the dependence of thrust with respect to the formation number. In that regard the same data has been re-plotted in Figure 14 on the formation number domain with each line pertaining to a specific frequency. This figure demonstrates that the optimum formation number is achieved around 4-5.5, which is in reasonable agreement with our model [1], [2]. As seen in this Figure the thrust value drops off rapidly as the jet deviates from the optimal value. The existence of this optimal formation number gives strong evidence for the vortex ring pinch off phenomenon. When the expelled jet first exits the orifice the boundary layer separation causes it to roll back on itself forming a vortex ring. As fluid is continually ejected from the orifice, a shear flow increasingly accumulate vorticity into the leading vortex ring, causing it to enlarge in size, velocity and most importantly impulse. As the formation number increases this effect also increases causing increased thrust until a limit is reached where the shear layer no longer

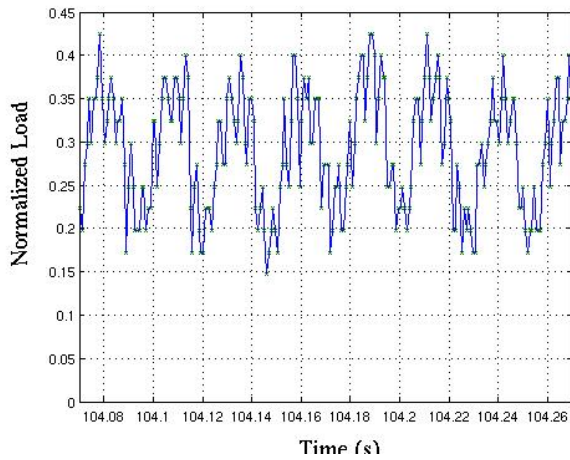


Fig. 11. Normalized load at 40 Hz actuation.

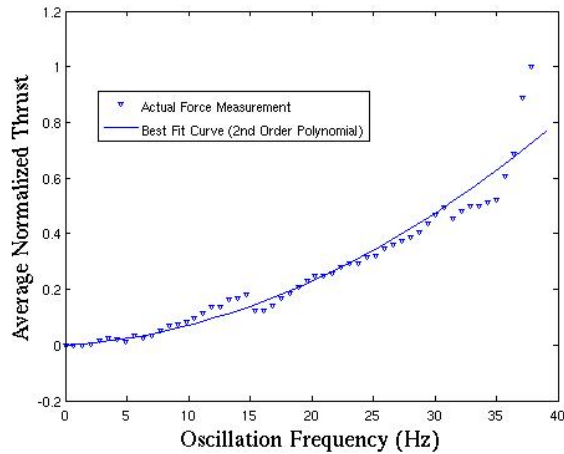


Fig. 12. Actuator thrust response (symbols) and fitted curve (solid line) in the frequency domain for $L/D = 3.93$.

has the velocity to fuel the growing vortex and the thrust again decreases. The pinch-off process was first observed and documented in Gharib *et al.* [13]. Numerical simulation of the same process (see Mohseni *et al.* [20]) is contrasted with the experiment in Figure 15.

It should be noted that all of the optimal thrust values discussed in this section so far were determined using an actuator whose Helmholtz cavity had a height of 2", and a diameter of 4". In an effort to characterize the thrust response to varying cavity geometry an identical experiment was run for a Helmholtz cavity with the same height but a smaller diameter of 2.5".

The smaller cavity was observed to have a similar dependency on the formation number, this can be seen in the thrust response curve for the smaller cavity on the formation number domain, depicted in Figure 16. However, a slightly different trend was observed with respect to the actuation frequency. At a characteristic peak frequency the thrust response of the actuator no longer increases with the square of the frequency, instead the thrust levels off and actually begins to decline. To

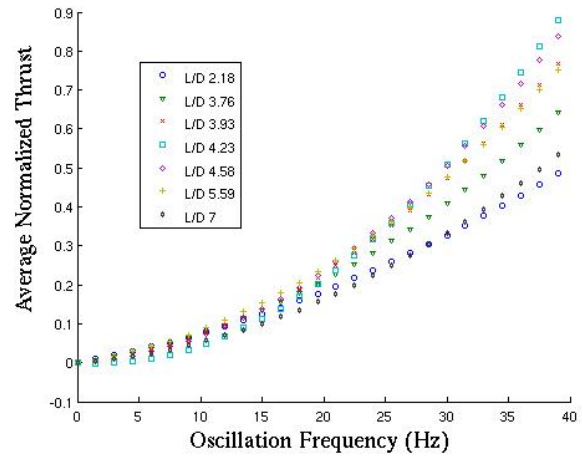


Fig. 13. Curve fitted actuator thrust response in the frequency domain for various formation numbers.

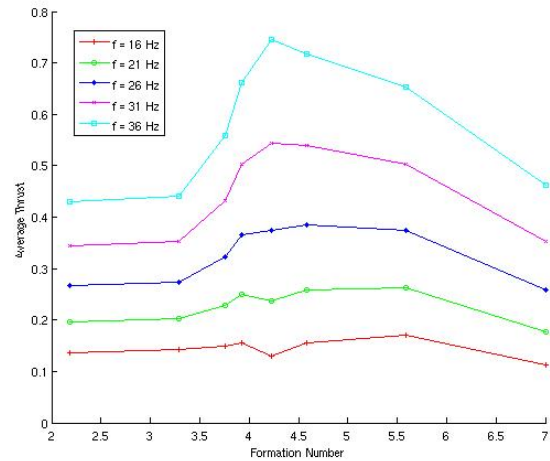


Fig. 14. Averaged normalized actuator thrust response in formation number domain.

demonstrate this phenomena, the thrust response curves for each cavity at a formation number of 4 have been depicted in Figure 17. There are several possible causes for this occurrence, cavitation inside the cavity and viscous effects are two plausible options. At the maximum stroke the smaller cavity has a narrow gap between the plunger and the cavity wall. As a result large shear is expected at high frequencies. This could explain the thrust drop at high frequencies in the smaller cavity.

B. Solenoid Stroke Data

One advantage of the setup being used to test the physical characteristics and limitations of the smaller solenoid actuators, is that it is entirely transparent. This allows us to use the setup for both flow visualization, as well as solenoid stroke testing. The ability to visualize the formation of vortex rings from the actuators gives crucial qualitative insight into the mechanism of ring formation, such as shear

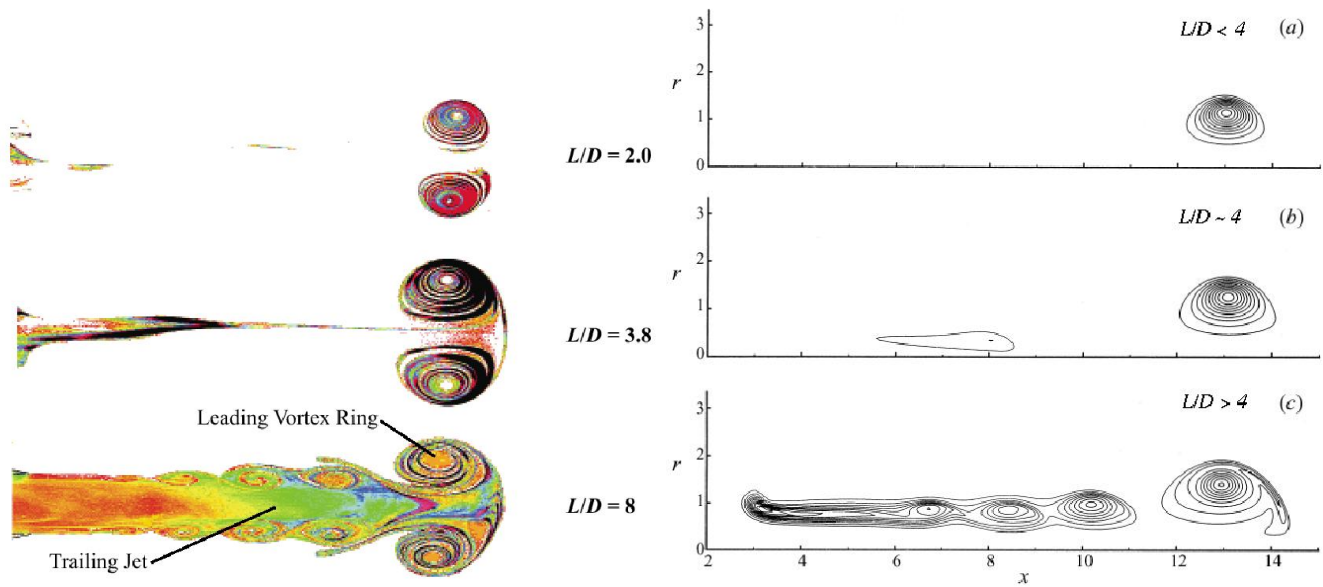


Fig. 15. (Left) Experimentally obtained fluid vorticity profiles during the vortex ring pinch-off process (for various L/D formation numbers) [13]. (Right) Numerical simulation of vortex ring formation at various formation numbers [20]. Only one half of the symmetric jet cross section is presented.

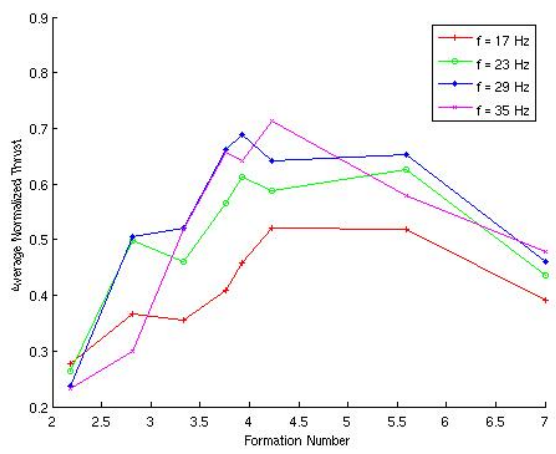


Fig. 16. Thrust response for the smaller cavity on the formation number domain

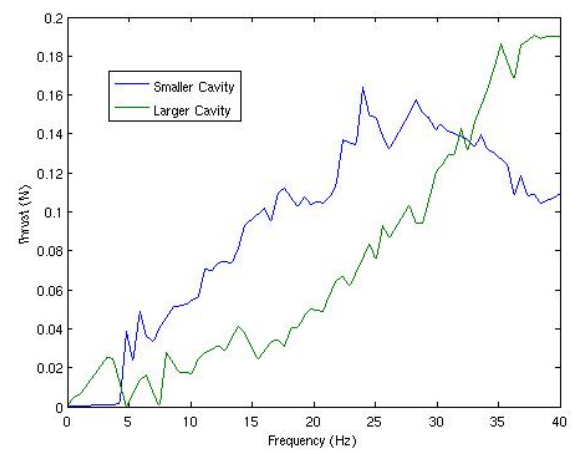
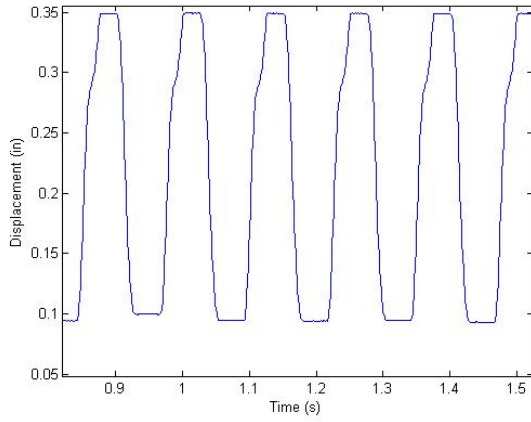


Fig. 17. Thrust response curve for two cavity diameters at L/D of 4

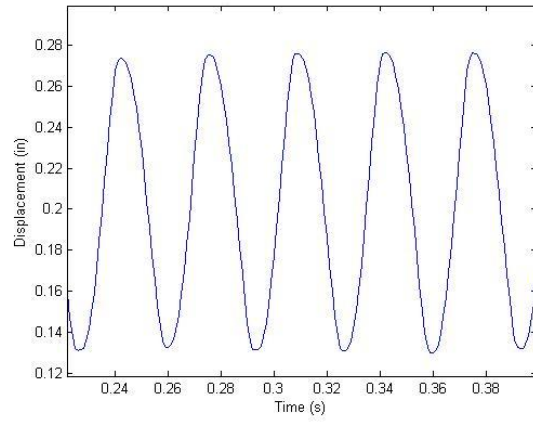
flow, ring velocity and ring thickness. This together with the quantitative thrust characteristics previously examined gives a better picture of the fluid interactions necessary for optimal thrust characteristics. In this case flow visualization is achieved by injecting dye into the cavity prior to activation. This allows the individual vortex rings to be observed as they are created. An example of one such visualization is depicted in Figure 18 where clear images of vortex formation are presented. In addition to providing qualitative insight into the fluid processes during the vortex ring formation, the solenoid actuator setup was used to quantitatively examine the stroke characteristics of the solenoid actuator under various load conditions.

The displacement profile of the solenoid plunger shows varying characteristics as the activation frequency is changed. At low frequencies (e.g. 7 Hz shown in Figure 19b), the

displacement very closely resembles its square wave input function during the ingestion phase while a more gradual change is observed during the expulsion phase. At these low frequencies, the solenoid has ample time to reach maximum deflection in both forward and reverse directions and a full stroke is achieved. As the frequency is increased, the reverse stroke is initiated before the forward stroke is completed, and the stroke length begins to decrease. At high frequencies (30 Hz shown in Figure 19b), the expulsion stroke is re-initiated before the reverse stroke is completed (the solenoid fails to return to rest position), and the total stroke length is further decreased. At 30 Hz, the stroke has decreased to 0.13 in. At these frequencies, the displacement function of the solenoid begins to resemble a sine wave as it has no time to rest in either the maximum or minimum position. This profile is more similar to that of the mechanical plunger actuator being



(a)



(b)

Fig. 19. Stroke profiles for solenoid actuator (a) at 7 Hz (b) at 30 Hz.

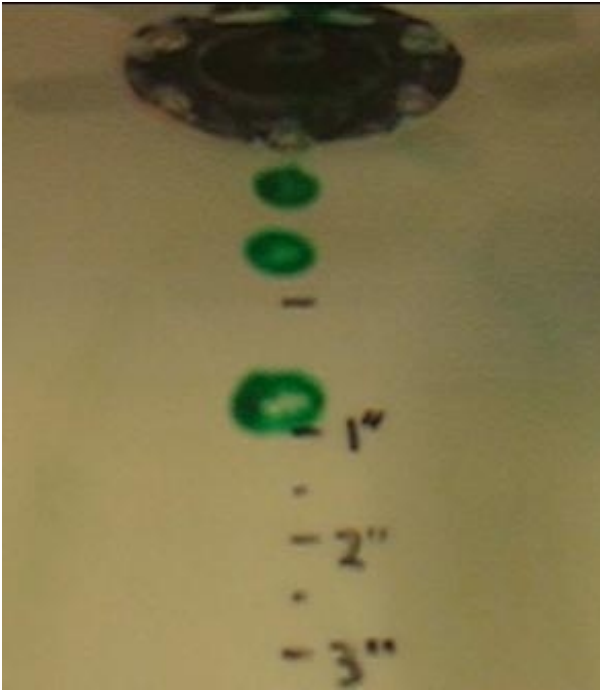


Fig. 18. Visualization of the vortex ring formation in a synthetic jet actuator.

used to find the optimal operation zone of a synthetic jet actuator. The mechanical plunger actuator is depicted in Figure 8. Continuing to increase the frequency will serve to decrease the stroke of the solenoid. To demonstrate this dependency, the stroke length of the actuator has been plotted with respect to the actuation frequency, for a given orifice diameter, in Figure 20. This graph shows that the actuation frequency plays an important role in defining the stroke characteristics of the solenoid plunger. While increasing frequency can increase the thrust produced from the synthetic jet actuator, it also serves to decrease the stroke length and thus decreases the volume of ejected fluid through the orifice. It should also be noted that by changing the orifice diameter or the elastic properties of the

membrane, the stroke response of the solenoid will change, as the pressure cycle inside the cavity and consequently solenoid loading will change.

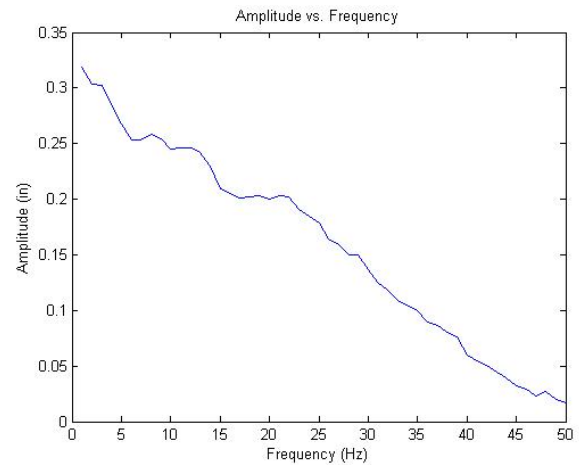


Fig. 20. Stroke length versus frequency of actuation.

IV. CONCLUSION AND FUTURE WORK

Thrust characteristics of a synthetic jet actuator for applications in propulsion and station keeping of underwater vehicles were studied. A new synthetic jet actuator was designed and built in order to easily control the actuation frequency, profile and cavity geometry. As predicted by our theoretical model, the empirical thrust shows a square dependency on the actuation frequency. It is observed that the measured thrust achieves a maximum value for formation numbers between 4 and 5.5, which is in agreement with our model. The solenoid stroke is observed to be a function of the loading and frequency of the actuation. At higher frequencies the solenoid stroke drops almost linearly with frequency. Future studies include investigation on the effect of design parameters such as the plunger stroke profile and cavity dimensions on the thrust generated, thus giving a scope for an optimal actuator design.

ACKNOWLEDGMENT

The authors would like to thank D. Lawrence for helpful discussions on thrust measurement system used in this investigation, and J. Burdick and A.M. Polsenberg Thomas for helpful discussions on control aspects of UUVs. The research in this paper was partially supported by the National Science Foundation contract IIS-0413300.

REFERENCES

- [1] K. Mohseni, "Pulsatile jets for unmanned underwater maneuvering," Chicago, Illinois, AIAA paper 2004-6386, 20-23 September 2004, 3rd AIAA Unmanned Unlimited Technical Conference, Workshop and Exhibit.
- [2] —, "Impulse extremization in synthetic jet actuators for underwater locomotion and maneuvering," in *submitted to the Proceedings of the 23rd International Conference on Offshore Mechanics and Arctic Engineering*. Vancouver, Canada, 20-25 June 2004, also published as a chapter in *Advances in Engineering Mechanics, Reflections and Outlooks: In Honor of Theodore Y.-T. Wu*, edited by A. T. Chwang, M. H. Teng and D. T. Valentine, World Scientific Publishing Company, 2005-.
- [3] M. Nixon and J. Messenger, Eds., *The Biology of Cephalopods*. Academic press, London, 1977.
- [4] R. O'Dor and D. Webber, "The constraints on cephalopods: Why squid aren't fish," *Canadian Journal of Zoology*, vol. 64, pp. 1591–1605, 1986.
- [5] —, "Invertebrate athletes: Trade-offs between transport efficiency and power density in cephalopod evolution," *Journal of Experimental Biology*, vol. 160, pp. 93–112, 1991.
- [6] J. Seikman, "On a pulsating jet from the end of a tube, with application to the propulsion of aquatic animals," *J. Fluid Mech*, vol. 15, pp. 399–418, 1963.
- [7] E. Trueman, "Motor performance of some cephalopods," *Journal of Experimental Biology*, vol. 49, pp. 495–505, 1968.
- [8] D. Weihs, "Periodic jet propulsion of aquatic creatures," in *Bewegungsphysiologie – Biomechanik*, W. Nachtigal, Ed., 1977, pp. 171–175.
- [9] E. DeMont and J. Gosline, "Mechanics of jet propulsion in the hydromedusan jellyfish, *polyorchis penicillatus*," *Journal of Experimental Biology*, vol. 134, pp. 347–361, 1988.
- [10] J. Dabiri, S. Colin, J. Costello, and M. Gharib, "Flow patterns generated by oblate medusan jellyfish: field measurements and laboratory analyses," *J. of Experimental Biology*, vol. 208, no. 7, pp. 1257–1265, 2005.
- [11] P. Krueger and M. Gharib, "The significance of vortex ring formation to the impulse and thrust of a starting jet," *Phys. Fluids*, vol. 15, no. 5, pp. 1271–1281, 2003.
- [12] —, "Thrust augmentation and vortex ring evolution in a fully pulsed jet," *AIAA J*, vol. 43, no. 4, pp. 792–801, 2005.
- [13] M. Gharib, E. Rambod, and K. Shariff, "A universal time scale for vortex ring formation," *J. Fluid Mech*, vol. 360, pp. 121–140, 1998.
- [14] K. Shariff and A. Leonard, "Vortex rings," *Ann. Rev. Fluid Mech.*, vol. 34, pp. 235–279, 1992.
- [15] R. Mittal, P. Rampunggoon, and H. S. Udaykumar, "Interaction of a synthetic jet with a flat plate boundary layer," AIAA paper 2001-2773, 2001.
- [16] L. Copperberg, L. Georgieva, C. Madsen, L. McCrann, and s. b. K. M. E. Thomas, "Summer project: Zero-mass change synthetic submarine maneuvering jets," August 2003.
- [17] M. Allgeier, K. DiFalco, D. Hunt, D. Maestas, S. Nauman, J. Poon, s. b. K. M. A. Shileikis, and S. Palo, "Senior design project: Remote Aquatic Vehicle," April 2004.
- [18] A. Thomas, J. Dabiri, K. Mohseni, and J. Burdick, "An experimental study of voice-coil driven synthetic jet propulsion for underwater vehicles," in *Proc. of the International Symposium on Unmanned Untethered Submersible Technology*, Durham, New Hampshire, August 21-24 2005.
- [19] A. Thomas, J. Burdick, and K. Mohseni, "An experimental study of voice-coil driven synthetic jet propulsion for underwater vehicles," in *Proceedings of the OCEANS 2005*. Washington, D.C.: MTS/IEEE, September 19-23 2005.
- [20] K. Mohseni, H. Ran, and T. Colonius, "Numerical experiments on vortex ring formation," *J. Fluid Mech*, vol. 430, pp. 267–282, 2001.